Rethinking phylogeographic structure and historical refugia in the rufous-capped babbler *Cyanoderma ruficeps* in light of range-wide genetic sampling and paleodistributional reconstructions

Peter A. Hosner[1,3*], Huatao Liu[2], A. Townsend Peterson[1], Robert G. Moyle[1]

[1] Biodiversity Institute, University of Kansas, Lawrence, Kansas 66045, USA

[2] School of Chemistry and Life Sciences, Guizhou Education University, Guiyang 550018, China

Abstract   Combining ecological niche modeling with phylogeography has become a popular approach to understand how historical climate changes have created and maintained population structure. However, methodological choices in geographic extents and environmental layer sets employed in modeling may affect results and interpretations profoundly. Here, we infer range-wide phylogeographic structure and model ecological niches of *Cyanoderma ruficeps*, and compare results to previous studies that examined this species across mainland China and Taiwan only. Use of dense taxon sampling of closely related species as outgroups question *C. ruficeps* monophyly. Furthermore, previously unsampled *C. ruficeps* populations from central Vietnam were closely related to disjunct western populations (Nepal, Tibet, Myanmar, Yunnan), rather than to geographically proximate populations in northern Vietnam and eastern China. Phylogeographic structure is more complex than previously appreciated; niche model projections to Last Glacial Maximum climate scenarios identified larger areas of suitable conditions than previous studies, but potential distributional limits differed markedly between climate models employed and were dependent upon interpretation of non-analogous historical climate scenarios. Previously identified population expansion across central China may result from colonization from refugial distributions during the Last Interglacial, rather than the Last Glacial Maximum, as previously understood [*Current Zoology* 61 (5): 901–909, 2015].

Keywords   Biogeography, Climate change, Ecological niche modeling, Southeast Asia, Pleistocene, Refugia

The rufous-capped babbler *Cyanoderma ruficeps* is a common bird species distributed across subtropical Asia including Nepal, northeastern India, northern Myanmar, northern Laos, Vietnam, mainland China, and the continental islands Hainan and Taiwan (Figs 1–2). It is found in broadleaf forest and second growth, and has a broad elevational distribution (near sea level to 3,200m). Generally, it is restricted to montane forests in the southern portion of its range. Until recently, *Cyanoderma* was included in the large and broadly distributed genus *Stachyris*, which was revealed as paraphyletic by molecular phylogenetic data (Cibois et al., 2002; Moyle et al., 2012). Subsequently, some authors have placed it in the genus *Stachyridopsis* (Cibois et al., 2002; Collar and Robson, 2007; Gill and Donsker, 2014), although *Cyanoderma* appears to have priority (Moyle et al., 2012). Its close relatives include *C. pyrrhops*, *C. ambigua*, and *C. rufifrons* (Moyle et al., 2012).

Three studies have examined phylogeographic relationships within *C. ruficeps* (Liu et al., 2012; Qu et al., 2014; Qu et al., 2015). Liu et al (2012) sequenced mitochondrial DNA from *C. ruficeps* populations from China (including Hainan), Taiwan, and Nepal, and identified five strongly supported clades: (1) Southwest (Nepal, Tibet, and Yunnan; *C. r. ruficeps* and *C. r. bhamoensis*); (2) Taiwan, *C. r. praecognita*; (3) Hainan, *C. r. goodsoni*; (4) Central (Sichuan, Guangxi, Guizhou; *C. r. davidi*, in part); and (5) Southeast (Guandong, Hunan, Jiangxi, Fujinan; *C. r. davidi*, in part). Central and southeast haplotypes were recovered from two sites in east-central China where the ranges of these two haplotype groups abut. Liu et al. (2012) produced a Last Glacial Maximum (LGM) ecological niche model (ENM) for *C. ruficeps* that showed highest suitability in the western portion of the range (Sichuan) and largely unsuitable conditions in Taiwan and Hainan. They proposed that isolation in Pleistocene refugia likely produced the observed distribution of genetic variation.

Qu et al. (2014) sequenced mitochondrial DNA and three nuclear genes for a subset of of Liu et al.'s (2012) samples. They restricted focus to mainland China, and recovered similar phylogeographic structure. Qu et al. (2014) produced niche models that differed markedly from Liu et al. (2012) with regards to potential distributions during the LGM. The Qu et al. (2014) models predicted limited areas of LGM suitability restricted to Hainan Island and the Qinling-Daba Mountains along China's southern border. Qu et al. (2014) also invoked refugia to explain the observed pattern of population differentiation.

Qu et al. (2015) sequenced 10 nuclear loci from *C. ruficeps* samples from across southern China and Taiwan. They identified three groups: (1) Taiwan, *C. r. praecognita*; (2) southeast (which included the central, southeast, and Hainan groups of Liu et al. 2012; *C. r. davidi and C. r. goodsoni*); and (3) southwest, *C. r. ruficeps* and *C. r. bhamoensis*. Qu et al. (2015) did not produce niche models, and instead favored physical barriers (ocean straights and topography) over isolation in climatic refugia to explain diversification in *C. ruficeps*.

Several aspects of *C. ruficeps* diversification remain uncertain. All previous studies sampled densely within China and Taiwan, which constitutes the bulk of the species' distribution. However, it is unknown whether unsampled populations (e.g. *C. r. pragana* and in Vietnam and Myanmar) represent distinct lineages or extensions of populations present in China. Furthermore, outgroup sampling has been sparse in previous studies: Liu et al. (2012) included *C. chrysaea* and *Mixornis gularis*, which fall in the same large clade as *C. ruficeps*, but are not particularly closely related (Moyle et al., 2012). Qu et al. (2015) did not specify which outgroup taxa were used in their analyses. Denser and more strategic outgroup sampling would allow tests of the integrity of current species limits and provide better rooting of the ingroup in phylogenetic analyses.

Ecological niche models presented by Liu et al. (2012) and Qu et al. (2014) were based on occurrence data from China and Taiwan only, and used political boundaries to define the background (or accessible area; **M**), for model calibration (Barve et al., 2011; Phillips et al., 2009). It remains unclear how adding occurrence data from throughout the species' range, and defining **M** based on biogeography and natural barriers would influence resulting niche models, although these factors are understood to affect model quality substantially (Peterson et al., 2011). Furthermore, Liu et al. (2012) and Qu et al. (2014) presented ENMs as continuous

models rather than thresholding them. Model thresholding allows more straightforward and comparable identification of suitable and unsuitable regions, and reduces effects of overfitting (Peterson and Nyári, 2007). Lastly, multiple general circulation models and time slices are now available for ENM projections, which may provide new views of environmental suitability.

Here, we build on the work of Liu et al. (2012), Qu et al. (2014), and Qu et al. (2015) by expanding geographic and taxonomic sampling in phylogeographic and ENM analyses. We have adjusted modeling methodologies to maximize our potential to estimate the full fundamental ecological niche, so that our model transfers and paleodistributional estimates are as accurate as possible. We compare these new results to their previous findings, and discuss implications for diversification across southern Asia.

1 Material and Methods

1.1 Sampling

Our genetic sampling focused on expanding geographic coverage of *C. ruficeps* to include populations outside China, as well as all other *Cyanoderma* species for denser outgroup comparisons. We extracted genomic DNA from 58 frozen or ethanol-preserved tissues of *C. ruficeps* samples collected across China, Vietnam, Myanmar, and Taiwan (supplemental information Table 1). From these tissues, we amplified and sequenced mitochondrial cytochrome *b* (Cyt *b*), NADH subunit 2 (ND2), and NADH subunit 3 (ND3); autosomal nuclear transforming growth factor intron 5, (TGFb52-5), and Z-linked nuclear muscle-specific kinase intron 2 (MUSK); the sequence matrix was built to be congruent with a recent higher-level study of babblers (Moyle et al., 2012). For additional details on primers and sequencing protocols, see Moyle et al. (2012). To this sequence matrix, we added Cyt *b* and cytochrome oxidase subunit 1 (*COI*) sequences from 138 individuals from Liu et al. (2012). We included all other *Cyanoderma* species as outgroups, and rooted ultimately to *Mixornis gularis* (Moyle et al., 2012, Liu et al., 2012), the final matrix with outgroups included sequences from 210 individuals.

1.2 Phylogenetic methods

We partitioned the concatenated DNA sequence matrix using PartitionFinder 1.1 (Lanfear et al., 2012); each codon position of each gene (for coding mitochondrial genes) and each intron were considered data blocks. We selected models of sequence evolution (JC, HKY, and GTR, each with and without estimated base frequencies,

proportion of invariant sites, and gamma-distributed rate heterogeneity) under the Bayesian Information Criterion (BIC) using the greedy search scheme.

We inferred phylogeny in Bayesian and maximum likelihood (ML) frameworks. For Bayesian analyses, we implemented MrBayes 3.2 (Ronquist et al., 2012) using partitions and models selected by PartitionFinder. We executed two 10 million generation MCMC runs, each with four chains. We sampled each run every 5,000 generations, and discarded the first 25% of samples as burn-in. Convergence was assessed in three ways: (1) examining the average standard deviation of split frequencies, (2) examining parameter convergence and effective sample size (all >200) in Tracer 1.5 (Rambaut and Drummond, 2007), and (3) examining topological convergence in AWTY (Nylander et al., 2008). We implemented ML analysis in RaxML 8.1 (Stamatakis, 2014), including a thorough ML search from 10 random starting trees under the GTRGAMMA model, and 500 thorough ML bootstraps using GTRGAMMA.

1.3 Ecological niche modeling

We gathered 829 unique georeferenced occurrences from the Global Biodiversity Information Facility (GBIF), which provides access to primary biodiversity data from scientific specimens and observations from citizen-science initiatives. Sampling was geographically biased, with high-densities of points across Taiwan, Bhutan, and Sikkim, and low densities elsewhere. To avoid over-fitting, we reduced density in these areas to match that in sparsely sampled areas across central China, leaving 79 points for model training and testing. We assumed an error rate (E) of 10% for these occurrence points, allowing for error in georeferencing. We developed a hypothesis of the accessible area (**M**) based on a 5° buffer of all points, but excluded areas inaccessible owing to deep ocean channels (e.g., the northern Philippines). To summarize environments, we used the following WorldClim bioclimatic layers: annual mean temperature, mean diurnal range, max temperature of warmest month, min temperature of coldest month, annual precipitation, precipitation of wettest quarter, and precipitation of driest quarter (Hijmans et al., 2005). For model calibration we implemented 100 replicate analyses in MaxEnt 3.3 (Phillips, 2006), each with up to 500 iterations and 10,000 background points, and used the median of the logistic output. For projections, we did not allow extrapolation or clamping, to avoid problems with model extrapolation (Owens et al., 2013). We evaluated the predictive power of the model with partial ROC approaches (Peterson et al., 2008), and thre-

sholded models at 90% and 100% training presence for visualization. Models calibrated on present-day layers were projected to LGM and Last Interglacial (LIG) climate scenarios drawn from the CCSM (Kiehl and Gent, 2004) and MIROC models (LGM only; Watanabe et al., 2011). Extrapolation to non-analogous paleo-climates was assessed using Mobility-Oriented Parity (MOP) for each model projection, calculated with 5% of the reference points sampled within **M** (Owens et al. 2013).

2 Results

2.1 Molecular phylogenetics

The aligned sequence matrix included 4,827 nucleotides and 776 phylogenetically informative characters (CO1: 1,237 bp, 193 informative sites; ND2: 1,041 bp, 243 informative sites; ND3: 351 bp, 89 informative sites; TGFb5-2: 533 bp, 20 informative sites; Cyt *b*: 1,143 bp, 216 informative sites; MUSK: 490 bp, 15 informative sites). PartitionFinder identified five partitions: ND2 and ND3 1st positions (HKY+I); Cyt *b* 1st position (K80+I); COI 1st position, TGFb5, and MUSK (K80+I+G); COI, ND2, ND3, and Cyt *b* 2nd positions (HKY+I); and COI, ND2, ND3, and Cyt *b* 3r^{d} positions (GTR+G). We identified five major geographic clades within *C. ruficeps*: (1) Taiwan; (2) southeastern China; (3) Hainan; (4) central China and northern Vietnam; and (5) Nepal, Tibet, Yunnan, northern Myanmar, and a disjunct population in central Vietnam (Fig 1). Different individuals from two localities in central China were found in both the central China/northern Vietnam clade and the southeastern China clade. The central Vietnam population was geographically isolated from, yet closely related to populations in Yunnan, Myanmar, Tibet, and Nepal, rather than to geographically proximate populations from northern Vietnam and southeastern China.

Phylogenetic results raise some doubt whether the five *C. ruficeps* clades form a natural group (Fig. 1). We found *C. pyrrhops* (Himalayas of W India and Pakistan) to be sister to western *C. ruficeps* populations (central Vietnam, Yunnan, Myanmar, Tibet, and Nepal), albeit with weak statistical support (0.66 posterior probability, 69% ML bootstrap support). *Cyanoderma ambigua* and *C. rufifrons* (strongly supported as sister taxa, 0.99 posterior probability and 81% ML bootstrap support) may also be sister to *C. pyrrhops* + western *C. ruficeps*. This topology had the highest likelihood among candidate topologies, but lacked bootstrap/statistical support.

2.2 Ecological niche modeling

Partial ROC scores were significant ($P < 0.0001$), indicating a strongly predictive model for *C. ruficeps*.

Present-day potential distribution largely mirrored raw occurrence points, and indicated that continuous, highly suitable environmental conditions exist throughout the species' extent of occurrence with two major exceptions: *C. ruficeps* was predicted to be locally absent from low elevations in central China, such as in the Sichuan Basin and the Yangtze River Basin, and from low elevations in central and southern Vietnam (Fig. 2). The potential

distribution also included two areas where *C. ruficeps* is thought to be absent and instead replaced by close relatives: the Himalayas west of central Nepal, and the Chin Hills of western Myanmar.

Projections of suitable environmental conditions to LGM climate scenarios from the CCSM and MIROC models produced similar results over much of Asia, with one major exception (Fig. 2B, 2C). Under the
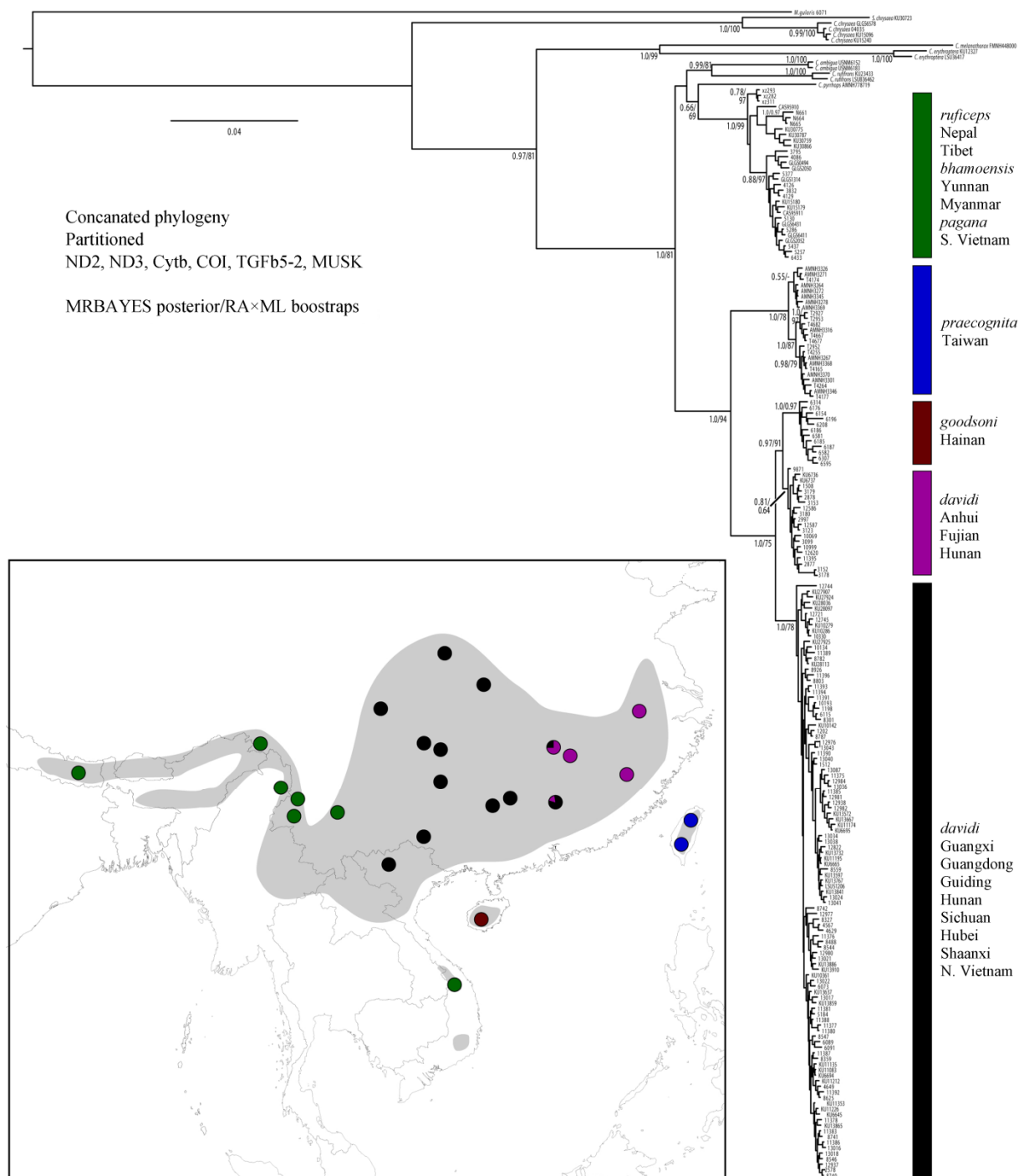

Fig. 1   Concatenated phylogeny of *C. ruficeps* and close relatives, clades are colored according to geographic location (inset, present-day distribution of *C. ruficeps* in gray), which are roughly concordant with subspecific designation

CCSM model, putative land bridges across the shallow Taiwan and Hainan Straits, which connected these islands to Mainland China during periods of low sea level, were reconstructed as unsuitable and constituted environmental barriers. In contrast, the MIROC model identified the Taiwan and Hainan Straits as suitable, refuting the idea of an environmental barrier. Areas of unsuitability in the CCSM LGM projections corresponded to areas of strict extrapolation as determined by the MOP analysis (Fig. 3), whereas MIROC LGM and LIG projections were largely free of extrapolation, at least within **M**. ENM projections to LIG conditions (Fig. 2D,
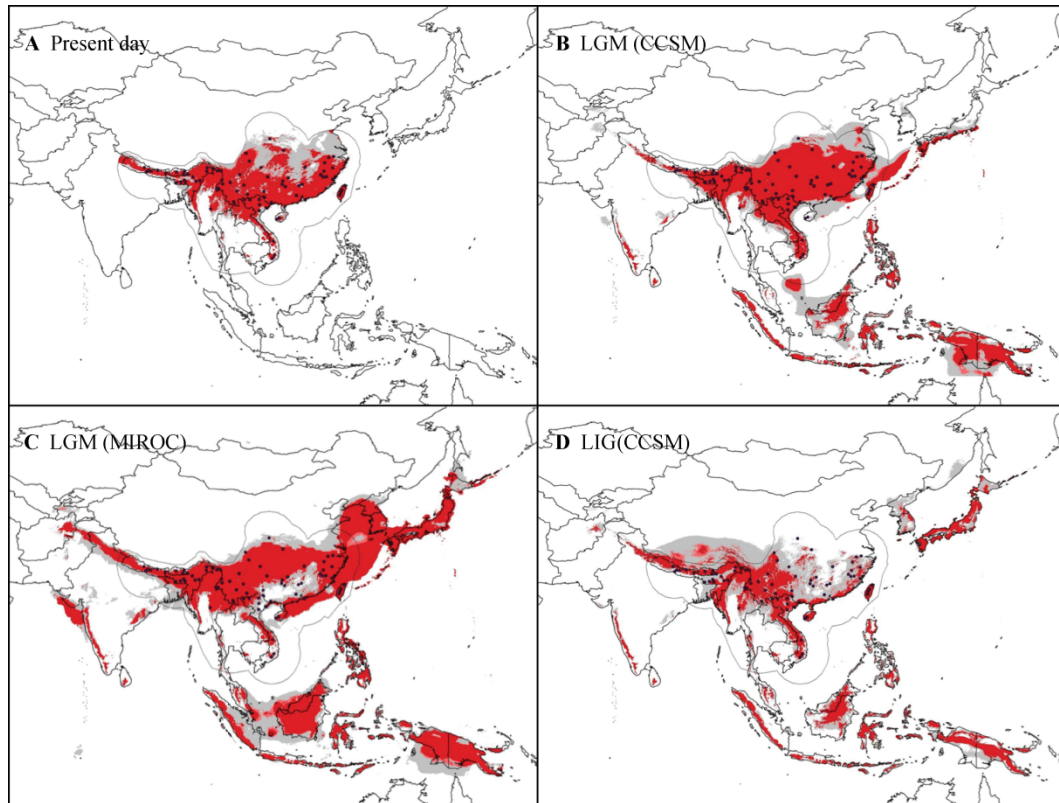

Fig. 2   Ecological niche model projections for *C. ruficeps*. Gray indicates 100% training presence, red indicates 90% training presence

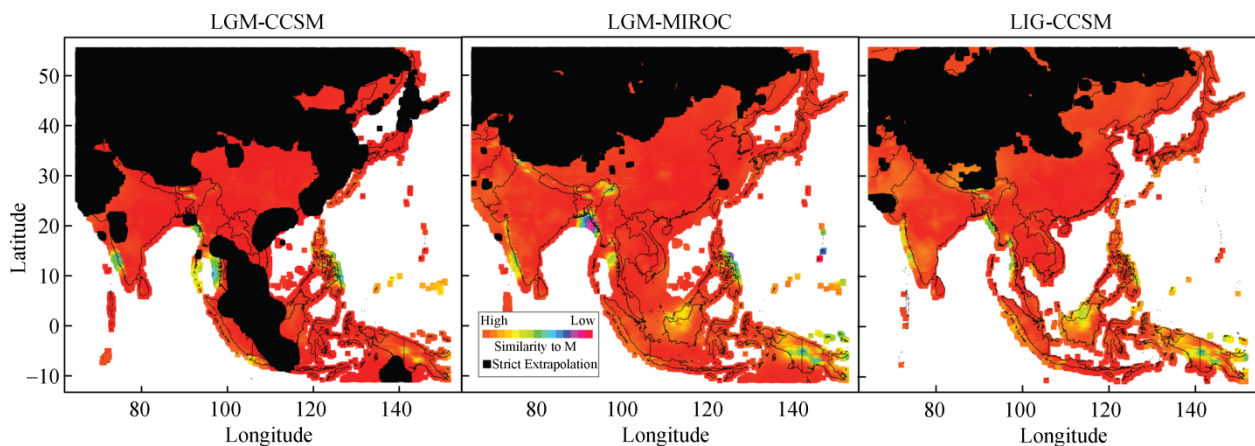Present day model is limited to within the training area (M), indicated by the gray line.

Fig. 3 MOP projections for the *C. ruficeps* training region (M) across Southeast Asia considering the 5% nearest points in multivariate space

LGM-CCSM projections show extensive areas within the *C. ruficeps* training region are strict extrapolation, falling outside of conditions observed within the training region. LGM-MIROC and LIG projections show little extrapolation within the training region.

CCSM available only) were largely similar to present-day conditions, except that environmentally suitable conditions in interior central China were much reduced.

3 Discussion

3.1 Phylogeography and niche models

Expansion of geographic and taxonomic sampling in phylogeographic analyses and paleodistributional models, along with a number of changes in model developments, yielded results that differ substantially from those of previous studies (Liu et al., 2012; Qu et al., 2014; Qu et al., 2015), and provide a template for discussion of potential factors (physical barriers and ecological tolerances) that may have influenced the evolution of *C. ruficeps* and other widespread Asian species.

Fundamentally, our results lead us to question *C. ruficeps* monophyly. The westernmost populations and the isolated population in central Vietnam (corresponding to subspecies *ruficeps*, *bhamoensis*, and *pagana*) formed a clade that was tentatively placed sister to *C. pyrrhops,* but with low support (69% BS, 0.66 PP). These taxa were in turn sister to *C. ambigua* and *C. rufifrons*, albeit again without support (< 50% BS, < 0.50 PP). None of these outgroup taxa was included in previous phylogeographic publications. Notably, additional ingroup samples also result in a slightly different topology from that inferred by Moyle et al. (2012), who found *C. pyrrhops* sister to all other *Cyanoderma* (although again, without strong support). Placement of *C. pyrrhops* is apparently unstable and dependent on taxon sampling. In this study, as in Moyle et al. (2012), *C. pyrrhops* sequence data were limited to mitochondrial DNA derived from a museum toepad; additional sequence data from the nuclear genome and additional analysis in a coalescent framework are needed to resolve its relationships with confidence.

The possibility that *C. pyrrhops* might disrupt the monophyly of *C. ruficeps* seems contradicted by plumage patterns: an overall drab plumage and a reddish cap unite all populations of *C. ruficeps*, whereas *C. pyrrhops* has a distinctive black cap and throat. However, a broader view of plumage patterns in *Cyanoderma* yields a different perspective. *Cyanoderma rufifrons* and *C. ambigua* share the general drab plumage and reddish cap of *C. ruficeps*, indicating that the plumage pattern that seems to unite populations of *C. ruficeps* is instead likely plesiomorphic for the whole clade.

Inclusion of genetic samples from Vietnam provided the most surprising results. Samples from the isolated population in the Central Highlands (Kon Tum Province)

were not closely related to those from northern Vietnam (Lao Cai Province), the latter being genetically similar to populations from across the border in southern China. Samples from the population in the Central Highlands of Vietnam were strongly supported as part of the clade sister to *C. pyrrhops*, which also includes *C. ruficeps* samples from Nepal, Tibet, Myanmar, and Yunnan. Another isolated population occurs in the southern Central Highlands of Vietnam (Lam Dong and Dak Lak Provinces), but samples were not available for this study.

ENM projections indicated that environmental suitability largely limits the present-day distribution of *C. ruficeps* (Fig. 2A). Only two relatively small suitable areas within our hypothesized **M** were unoccupied by *C. ruficeps*: the Western Himalayas (where *C. ruficeps* is replaced by closely related *C. pyrrhops*) and the Chin Hills of western Myanmar, where *S. ruficeps* is by replaced by closely related *C. ambigua.* Cross-prediction of ecological niches among closely related taxa is expected under niche conservatism (Peterson, 1999). Population divergence within the present-day distribution of *C. ruficeps* and allies is thus unrelated to present-day environmental barriers, and rather is likely driven by historical factors such as physical barriers (rivers, topography, or marine barriers) or changing environmental suitability during the tumultuous Plio-Pleistocene climate cycles.

Projecting *C. ruficeps* ENMs to Pleistocene climate scenarios highlighted important challenges in paleodistributional inference and interpretation. The CCSM LGM projection inferred a suitability gap across the Taiwan Strait, supporting the idea that the combination of a climate-driven barrier during glacial maxima and a physical barrier during interglacials is responsible for isolation and genetic divergence between populations in Taiwan and Mainland China (Fig. 2B). However, this area of unsuitability was coincident with an area of non-analogous climates. That is, from ENMs, it is uncertain and unknowable whether these conditions, not represented within the present-day **M**, were actually unsuitable to *C. ruficeps*, or whether these conditions would be suitable if *C. ruficeps* had access to them.

MIROC LGM projection supported an alternate scenario, wherein suitable and analogous to present-day environments were continuous across the Taiwan Strait, and thus additional isolation mechanisms would be needed (Fig. 2C). Hence, consideration of alternate climate models and model transferability factor in the interpretation of *C. ruficeps* paleodistribution. None of our paleodistributional models could offer climate-based

explanations for the separation of the major mainland clades of *C. ruficeps*, or for the disjunct distribution of the central Vietnam population (Fig. 2B–2C).

3.2   Comparison to previous results

Our phylogenetic and paleodistribution results were strikingly different from those of other recent studies of *C. ruficeps*. Phylogeographic differences resulted from inclusion of key additional populations and outgroups, and differences were minor where sampling overlapped. ENM results predicted broad areas of suitable conditions across much of the species' range at the LGM, whereas Liu et al. (2012) and Qu et al. (2014) predicted mostly unsuitable conditions with small pockets of high suitability. The exact causes of these differences are hard to identify, as we adjusted numerous methodological choices to bring ENM methods in line with a current conceptual and empirical synthesis (Peterson et al., 2011). Liu et al. (2012) and Qu et al. (2014) restricted their occurrence data and LGM projections to a subset of the range of *C. ruficeps*, which can yield in an incomplete view of suitable areas. These effects can be observed in both of their LGM projections, which showed areas of high suitability truncated by the political border of China. Population distributions, dispersal hypotheses, and geographic features, rather than political boundaries, should bound ENM calibration areas (Barve et al., 2011; Phillips et al., 2009).

Our use of two different climate models for LGM model transfers examined how variation in knowledge of LGM conditions might influence results. Although the two climate models agreed over large parts of *C. ruficeps'* distribution, important differences between them yield conflicting historical inferences. These results suggest that caution is warranted in strict interpretation of paleodistributional projections of ENMs.

Similarly, examining LIG conditions in addition to LGM conditions adds important insights to understanding *C. ruficeps* distributional ecology. Our broad LGM projections would seem to contradict the Qu et al.'s (2014) conclusion that long-term environmental suitability influences genetic diversity in *C. ruficeps*. However, our LIG model projection showed reduced suitability in areas of reduced genetic diversity reported by Qu et al. (2014), such that reduction of environmental suitability in the LIG, rather than the LGM, may have driven these observed patterns.

Because *C. ruficeps* is common and widely distributed, with populations that exhibit strong genetic structure, it will likely continue to be a key species in understanding avian biogeography and evolution in Southeast Asia.

Future studies must address the possible paraphyly suggested by this study, and determine whether populations featured in recent studies indeed form natural groups. Wider geographic sampling is also needed, both to determine historical relationships of unsampled populations (e.g., in the southern Central Highlands of Vietnam), and to investigate areas that may reveal zones of overlap or admixture between clades where their distributions approach.

References

Barve N, Barve V, Jiménez-Valverde A, Lira-Noriega A, Maher SP et al., 2011. The crucial role of the accessible area in ecological niche modeling and species distribution modeling. Ecol. Model. 222: 1810–1819.

Cibois A, Kalyakin MV, Han LX, Pasquet E, 2002. Molecular phylogenetics of babblers (Timaliidae): Revaluation of the genera *Yuhina* and *Stachyris*. J. Avian Biol. 33: 380–390.

Collar NJ, Robson C, 2007. Family Timaliidae (Babblers). In: Del Hoyo J, Elliott A, Christie DA eds. Handbook of the Birds of the World. Vol. 12: *Picathartes* to Tits and Chicadees. Barcelona: Lynx Ediciones, 70–291.

Gill F, Donsker D, 2014. IOC World Bird Names (version 4.0). http://www. worldbirdnames.org.

Hijmans RJ, Cameron SE, Parra JL, 2005. Very high resolution interpolated climate surfaces for global land areas. Int. J. Climatol. 25: 1965–1978.

Kiehl JT, Gent PR, 2004. The community climate system model, Version 2. J. Climate 17: 3666–3682.

Lanfear R, Calcott B, Ho SYW, Guindon S, 2012. PartitionFinder: Combined selection of partitioning schemes and substitution models for phylogenetic analyses. Mol. Biol. Evol. 29: 1695–1701.

Liu H, Wang W, Song G, Qu Y, Li SH et al., 2012. Interpreting the process behind endemism in China by integrating the phylogeography and ecological niche models of the *Stachyridopsis ruficeps*. PLoS ONE 7: e46761.

Moyle RG, Andersen MJ, Oliveros CH, Steinheimer FD, Reddy S, 2012. Phylogeny and biogeography of the core babblers (Aves: Timaliidae). Syst. Biol. 61: 631–651.

Nylander JAA, Wilgenbusch JC, Warren DL, Swofford DL, 2008. AWTY (are we there yet?): A system for graphical exploration of MCMC convergence in Bayesian phylogenetics. Bioinformatics 24: 581–583.

Owens HL, Campbell LP, Dornak L, Saupe E, Barve N et al., 2013. Constraints on interpretation of ecological niche models by limited environmental ranges on calibration areas. Ecol.

Model. 263: 10–18.

Peterson AT, 1999. Conservatism of ecological niches in evolutionary time. Science 285: 1265–1267.

Peterson AT, Nyári ÁS, 2007. Ecological niche conservatism and Pleistocene refugia in the thrush-like mourner *Schiffornis* sp. in the Neotropics. Evolution 62: 173–183.

Peterson AT, Papeş M, Soberón J, 2008. Rethinking receiver operating characteristic analysis applications in ecological niche modeling. Ecol. Model. 213: 63–72.

Peterson AT, Soberón J, Pearson RG, Anderson RP, Martínez-Meyer E et al., 2011. Ecological Niches and Geographic Distributions. Princeton: Princeton University Press.

Phillips SJ, Dudík M, Elith J, Graham CH, Lehmann A et al., 2009. Sample selection bias and presence-only distribution models: Implications for background and pseudo-absence data. Ecol. Appl. 19: 181–197.

Qu YH, Ericson PGP, Quan Q, Song G, Zhang R et al., 2014. Long-term isolation and stability explain high genetic diversity in the Eastern Himalaya. Mol. Ecol. 23: 705–720.

Qu Y, Song G, Gao B, Quan Q, Ericson PGP et al., 2015. The influence of geological events on the endemism of East Asian birds studied through comparative phylogeography. J. Biogeogr. 42: 179–192.

Rambaut A, Drummond AJ, 2007. Tracer version 1.5. available from http://beast.bio.ed.ac.uk.

Ronquist F, Teslenko M, van der Mark P, Ayres DL, Darling A et al., 2012. MrBayes 3.2: Efficient Bayesian phylogenetic inference and model choice across a large model space. Syst. Biol. 61: 539–542.

Stamatakis A, 2014. RAxML version 8: A tool for phylogenetic analysis and post-analysis of large phylogenies. Bioinformatics 30: 1312–1313.

Watanabe S, Hajima T, Sudo K, Nagashima T, Takemura T et al., 2011. MIROC-ESM 2010: Model description and basic results of CMIP5-20c3m experiments. Geosci. Model Dev. 4:, 845–872.

Supplemental Table S1   Tissue samples and voucher specimens newly sequenced for this study

Institution	Voucher number	Species	Geographical identity	State
USNM	6152	*Cyanoderma ambigua*	Myanmar	
USNM	6183	*Cyanoderma ambigua*	Myanmar	
KU	15096	*Cyanoderma chrysaea*	Myanmar	Ma Jed
KU	15240	*Cyanoderma chrysaea*	Myanmar	Jed Lwe
KU	30723	*Cyanoderma chrysaea*	Vietnam	Kon Tum
AMNH	778719	*Cyanoderma pyrrhops*	India	Uttar Pradesh
AMNH	3264	*Cyanoderma ruficeps*	China	Taiwan
AMNH	3267	*Cyanoderma ruficeps*	China	Taiwan
AMNH	3267	*Cyanoderma ruficeps*	China	Taiwan
AMNH	3271	*Cyanoderma ruficeps*	China	Taiwan
AMNH	3272	*Cyanoderma ruficeps*	China	Taiwan
AMNH	3278	*Cyanoderma ruficeps*	China	Taiwan
AMNH	3301	*Cyanoderma ruficeps*	China	Taiwan
AMNH	3316	*Cyanoderma ruficeps*	China	Taiwan
AMNH	3326	*Cyanoderma ruficeps*	China	Taiwan
AMNH	3345	*Cyanoderma ruficeps*	China	Taiwan
AMNH	3346	*Cyanoderma ruficeps*	China	Taiwan
AMNH	3368	*Cyanoderma ruficeps*	China	Taiwan
AMNH	3369	*Cyanoderma ruficeps*	China	Taiwan
AMNH	3370	*Cyanoderma ruficeps*	China	Taiwan
KU	6645	*Cyanoderma ruficeps*	China	Hunan
KU	6665	*Cyanoderma ruficeps*	China	Hunan
KU	6694	*Cyanoderma ruficeps*	China	Hunan
KU	6695	*Cyanoderma ruficeps*	China	Hunan
KU	6736	*Cyanoderma ruficeps*	China	Hunan
KU	6737	*Cyanoderma ruficeps*	China	Hunan
KU	10142	*Cyanoderma ruficeps*	China	Guangxi

Institution	voucher number	species	Geographical identity	State
KU	10279	*Cyanoderma ruficeps*	China	Guangxi
KU	10286	*Cyanoderma ruficeps*	China	Guangxi
KU	10330	*Cyanoderma ruficeps*	China	Guangxi
KU	10361	*Cyanoderma ruficeps*	China	Guangxi
KU	11083	*Cyanoderma ruficeps*	China	Guizhou
KU	11135	*Cyanoderma ruficeps*	China	Guizhou
KU	11174	*Cyanoderma ruficeps*	China	Guizhou
KU	11195	*Cyanoderma ruficeps*	China	Guizhou
KU	11212	*Cyanoderma ruficeps*	China	Guizhou
KU	11226	*Cyanoderma ruficeps*	China	Guizhou
KU	11353	*Cyanoderma ruficeps*	China	Guizhou
KU	13572	*Cyanoderma ruficeps*	China	Guizhou
KU	13597	*Cyanoderma ruficeps*	China	Guizhou
KU	13637	*Cyanoderma ruficeps*	China	Guizhou
KU	13667	*Cyanoderma ruficeps*	China	Guizhou
KU	13732	*Cyanoderma ruficeps*	China	Guizhou
KU	13767	*Cyanoderma ruficeps*	China	Guizhou
KU	13841	*Cyanoderma ruficeps*	China	Guizhou
KU	13859	*Cyanoderma ruficeps*	China	Guizhou
KU	13865	*Cyanoderma ruficeps*	China	Guizhou
KU	13886	*Cyanoderma ruficeps*	China	Guizhou
KU	13910	*Cyanoderma ruficeps*	China	Guizhou
KU	15179	*Cyanoderma ruficeps*	Myanmar	Jed Lwe
KU	15180	*Cyanoderma ruficeps*	Myanmar	Jed Lwe
KU	27907	*Cyanoderma ruficeps*	Vietnam	Lao Cai
KU	27924	*Cyanoderma ruficeps*	Vietnam	Lao Cai
KU	27925	*Cyanoderma ruficeps*	Vietnam	Lao Cai
KU	28036	*Cyanoderma ruficeps*	Vietnam	Lao Cai
KU	28097	*Cyanoderma ruficeps*	Vietnam	Lao Cai
KU	28113	*Cyanoderma ruficeps*	Vietnam	Lao Cai
KU	30759	*Cyanoderma ruficeps*	Vietnam	Kon Tum
KU	30775	*Cyanoderma ruficeps*	Vietnam	Kon Tum
KU	30787	*Cyanoderma ruficeps*	Vietnam	Kon Tum
KU	30866	*Cyanoderma ruficeps*	Vietnam	Kon Tum
LSUMZ	51206	*Cyanoderma ruficeps*	China	Guandong
CAS	95910	*Cyanoderma ruficeps*	China	Yunnan
CAS	95911	*Cyanoderma ruficeps*	China	Yunnan
KU	23433	*Cyanoderma rufifrons*	Vietnam	Dai Bien
LSUMZ	B36462	*Cyanoderma rufifrons*	Malaysia	Sabah
KU	12327	*Stachyris erythroptera*	Malaysia	Sarawak
LSUMZ	B36417	*Stachyris erythroptera*	Malaysia	Sabah
AMNH	448000	*Stachyris melanothorax*	Indonesia	Java

Additional samples were published previously in Moyle et al. (2012) and Liu et al. (2012).